

93-301



ОБЪЕДИНЕННЫЙ  
ИНСТИТУТ  
ЯДЕРНЫХ  
ИССЛЕДОВАНИЙ  
ДУБНА

301-93

E6-93-301

J.Rak<sup>1</sup>, V.B.Brudanin, V.G.Egorov, V.E.Kovalenko,  
Ch.Briançon<sup>2</sup>, J.S.Dionisio<sup>2</sup>, Ch.Vieu<sup>2</sup>

DETERMINATION OF THE COMPTON  
SUPPRESSION EFFICIENCY  
OF Ge-BGO DETECTORS  
IN LOW  $\gamma$ -RAY ENERGY REGION

Submitted to «NIM»

<sup>1</sup> At present Nuclear Physics Institute of Academy of Sciences  
of Czech Republic, Řež near Prague, Czech Republic

<sup>2</sup> Centre de Spectrométrie Nucleaire et de Spectrométrie de Masse,  
Orsay, France

1993

# 1. Introduction

Recently, many experiments using Compton suppression spectrometers (CSS) have been carried out. Large spherical CSS arrays have usually been used in advanced nuclear structure experiments and precise  $\gamma$ -ray spectroscopy studies (TESSA, NORDBALL, EUROGAM etc.) [1].

The first descriptions of such devices were given in the sixtieth by Kantale and Suominen [2], Michaelis [3] and others (see also [4]). The first CSS, usually  $Ge(Li)$  detector surrounded with plastic and/or NaI scintillator, were developed in the field of neutron capture  $\gamma$ -ray spectroscopy. Since then new scintillator materials have been developed, particularly BGO and  $BaF_2$ , and nowadays it opened wide possibilities in nuclear studies.

Precise computational methods based on Monte Carlo calculation (EGS [6], GEANT [7], see also [8]) have been developed. These methods facilitate to predict the response function of various configurations of CSS with high accuracy. In such manner the optimal shape and the dimension of manted detector can be calculated. One has also obviously to take into account the best performance/cost ratio for a given experimental set up.

## 2. The choice of convenient program tool for Monte Carlo simulation

The CERN's product GEANT [7] and the EGS4 (Electron-Gamma-Shower) [6] system of the computer code written at the Stanford Linear Accelerator Center was tested. The GEANT and EGS4 are general purpose packages for the Monte Carlo simulation of the transport of particles with energies above 10 keV up to several TeV. GEANT code provides the possibility to study the transport of approximately 100 types of particles ( $e^-$ ,  $e^+$ ,  $p$ ,  $n$ ,  $\pi^{0,+,-}$ ,  $\nu_e, \dots$ , heavy ions). The EGS4 allows to describe the transport of  $e^-$ ,  $e^+$  and  $\gamma$ .

For the comparison of the above mentioned program tools performance the response function of simple detector were simulated. The detector was compounded from 10 mm and 2 mm of plastic scintillator slabs separated by 10 mm Pb slab. The spectra of the energy deposited in those slabs by 2 MeV photons passing through such detector are shown on Fig. 1. The left Figures represent the results of GEANT simulation and the right ones the EGS4 simulation.

## GEANT - EGS4 comp. 2 MeV gamma

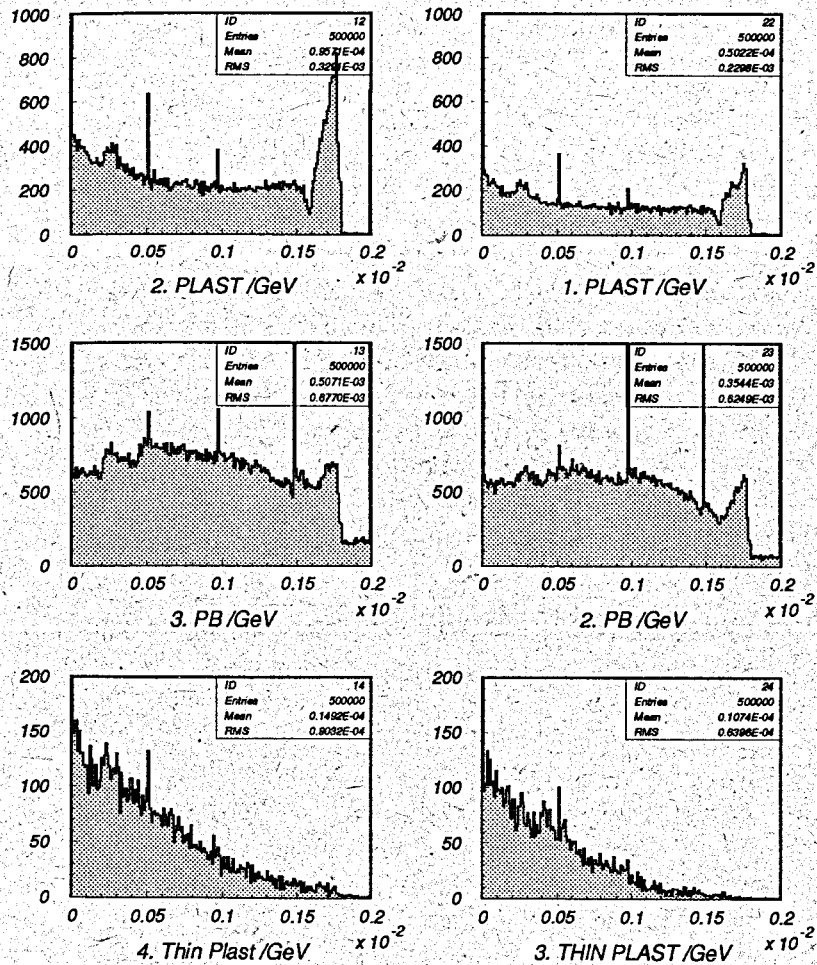


Figure 1: GEANT and EGS4 Monte Carlo simulation. 2 MeV  $\gamma$  pass through the detector compounded from 10 mm and 2 mm slab of plastic scintillator separated by 10 mm Pb slab.

Since the agreement of those results is good enough, the more simple code EGS4 has been chosen. There are involved almost all nowadays known physical processes of photon and electron interaction (Photoelectric effect, Compton scattering, Pair production and Coherent scattering for photons and Coulomb,  $(e^+e^-)$ ,  $(e^+e^+)$  scattering, Bremsstrahlung production, Positron annihilation in flight and at rest etc.)

### 3. The Ge-BGO spectrometer

During the last few years the experiments at the IPN MP-tandem accelerator in Orsay have been extensively carried out [11, 12]. In these experiments the high spin nuclear levels ( $I \approx 50 \hbar$ ) were investigated. Since the transitions between excited states belong mainly to low  $\gamma$ -rays energy region, the region 20..100 keV provides the most important information. Complex energy structure of  $\gamma$ -spectra in this region demands high sensitivity of gamma spectrometer. From this reason the CSS shown on Fig. 2 has been included and studied. The calculation of the response function and the Compton suppression factor defined as the ratio of the unsuppressed to the suppressed spectrum were computed out. Experimental response function has been measured with high purity Ge detector GMX-20190-S with crystal in 51.1 mm diameter, 46.6 mm length and relative efficiency 20.4% and FWHM 2.31 keV at 1332 keV ( $^{60}\text{Co}$ ). The configuration without small BGO cylinder (BCB) has been analysed. The  $^{88}\text{Y}$  and  $^{137}\text{Cs}$  sources have been placed at 20 cm from front of the Ge detector. The experimental data with the Monte Carlo predictions are shown on Fig. 3.

The inactive layers which mostly attenuate the suppression efficiency are following:

- the aluminum envelope surrounding the Ge crystal
- constructive material keeping the scintillator
- contact region on the surface of Ge crystal (usually the thickness of 600  $\mu\text{m}$ ).

The influence of inactive layers on the suppression factor is evident from the figures. This fact is important and in order to obtain results with sufficient accuracy the absorption of Compton scattered photons in dead layers cannot be neglected. The calculations performed without taking into

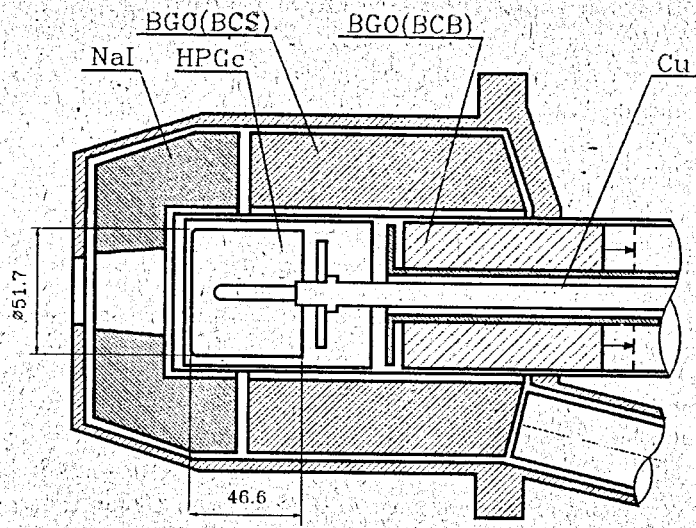


Figure 2: The scheme of the Compton suppression detector designed by Harshaw, Holland intended to EUROGAM experiment. The CSS is made from a mantled BGO cylinder (BCS), a conical 1 cm nose of NaI and small BGO cylinder (BCB) placed behind Ge detector.

Table 1: Comparison of experimental and calculated Compton suppression factor for the geometry of the CSS shown on Fig.2. The mean value is determined for the energy region above 100keV up to 650 keV for  $^{137}\text{Cs}$  and up to 1750 keV for  $^{88}\text{Y}$ . The maximum value was determined near the Compton edge.

		Mean	Max
$^{88}\text{Y}$	Exper.	3.43 (0.09)	5.80 (0.3)
	Solid line	3.49 (0.11)	5.57 (0.1)
	Dashed line	6.60 (0.12)	15.20 (0.5)
$^{137}\text{Cs}$	Exper.	4.01 (0.24)	6.43 (0.2)
	Solid line	3.60 (0.33)	5.50 (0.07)
	Dashed line	14.22 (0.88)	38.12 (0.9)

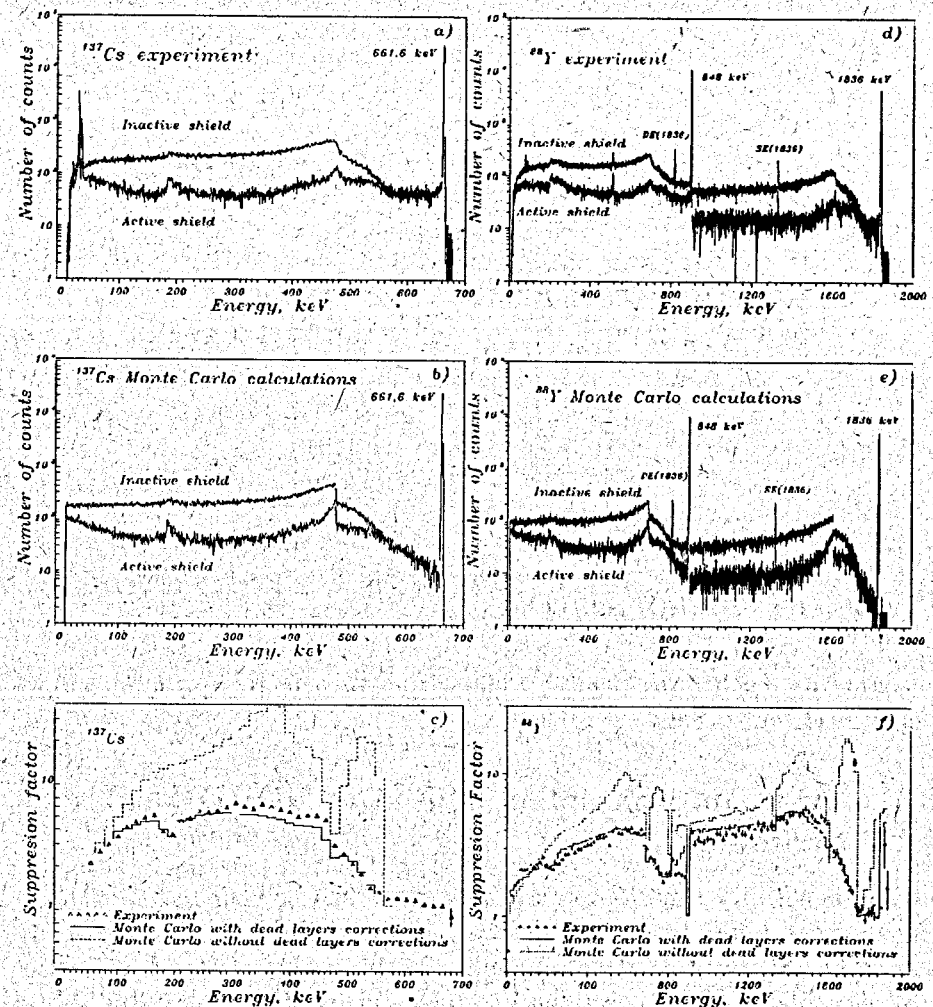


Figure 3: The measured spectrum of  $^{137}\text{Cs}$  with CSS shown on Fig.2 , (part (a)). The Monte Carlo predicted spectrum for the same configuration (part (b)). The measured spectrum of  $^{88}\text{Y}$  with CSS shown on Fig.1 , (part (d)). The Monte Carlo predicted spectrum for the same configuration (part (e)). The Compton suppression factor as function of the energy. The dashed line represents the simple calculation without taking into account the inactive (dead) layers. The solid line represents the results calculated with taking into account the dead layers surrounding the crystals. Part (c) shows the results of the calculations for the source  $^{137}\text{Cs}$  and part (f) for  $^{88}\text{Y}$ .

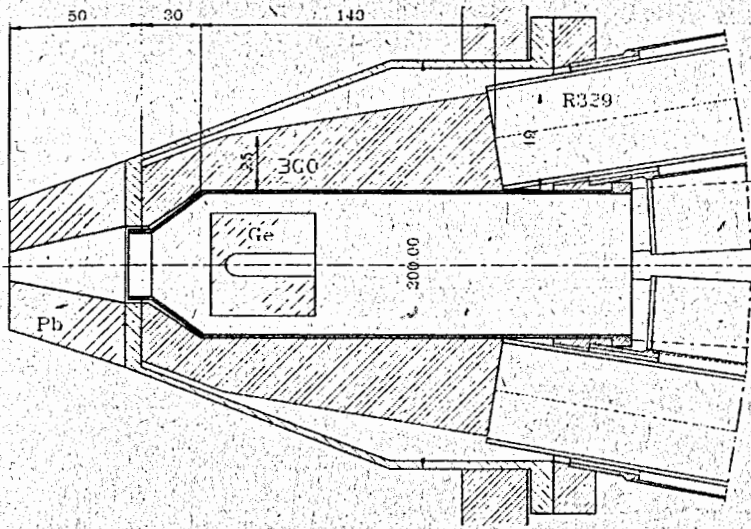


Figure 4: The scheme of the Compton suppression spectrometer designed in Niels Bohr Institute (NORDBALL).

account the dead layers overrates the suppression factor in some energy region over four times (see Table 1).

### 3.1. Anticompton detector used in NORDBALL experiment

Fig. 3. and Table 1. show a satisfactory agreement between measured and calculated response function of detector drawn on Fig. 2. It has provided a good test of our calculation reliability. The results of measurement with CSS designed at the Niels Bohr Institute and used in the NORDBALL array (Fig. 4) have been used too. In Ref. [9] the results of the Monte Carlo simulation based on EGS code are discussed. The authors came to the conclusion that the comparison of the Monte Carlo calculations with experimental results was not satisfactory, since the calculated suppression factor near the Compton edge is approximately two times larger (20-30) than the measured one (12) with the  $^{60}\text{Co}$  source. They brought out a list of three factors, which might cause such disagreement

Table 2: The comparison of experimental and calculated Compton suppression factor for CSS from Fig.4. The mean value is determined for the energy region above 100 keV up to 650 keV for  $^{137}\text{Cs}$  and up to 1200 keV for  $^{60}\text{Co}$ . The maximum value is determined near Compton edge. Monte Carlo (M.C.) real and M.C. simple comments the calculation with resp. without taking into account the absorption in dead layers.

		Mean	Max
$^{60}\text{Co}$	Exper.	6.74	12.18
	M.C. real	7.31 (0.17)	12.32 (0.36)
	M.C. simple	16.17 (0.14)	46.92 (2.4)
$^{137}\text{Cs}$	Exper.	6.99	12.69
	M.C. real	6.31 (0.49)	10.18 (0.14)

- reduced detection efficiency of the BGO shield or imperfect veto signal
- escape of electrons from the outside regions of the Ge detector
- imperfection of the Ge detector reflected in incomplete charge collection.

All these factors may cause the discrepancies between calculated and measured suppression factors. From our analysis it became evident that the addition of another factor, probably most significant, will be useful. This factor includes the absorption of scattered  $\gamma$ -rays in the surrounding inactive layers. The calculations of response function of the detector described in [9] with and without taking into account the absorption in dead layers have been carried out. In the first case the value of 47 for the suppression factor near the Compton edge was obtained and it is in large disagreement with the experimental value (see Table 2). On the other hand the calculations performed with taking into account the dead layers (described above) give a satisfactory agreement.

The comparison between measured and calculated suppression factors for NBI CSS from Fig. 4 are shown on Fig. 5.

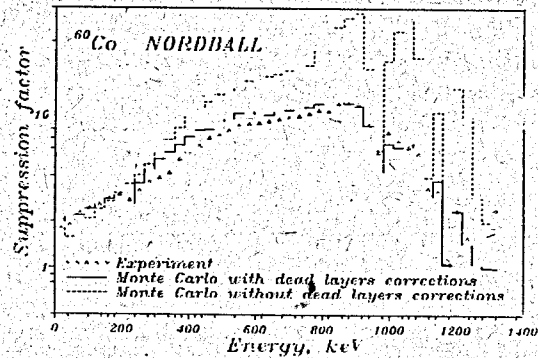


Figure 5: The measured and calculated suppression factors for CSS designed on NBI.

## 4. Results

### 4.1. Calculation of backward BGO cylinder suppression efficiency

Since the main contribution to the low energy region originates from small angle scattered  $\gamma$ -rays the possibility to place small BGO cylinder directly inside the Ge detector envelope (marked as BCB on Fig. 2) was considered. Using the calculations described above we tried to estimate the advantage of using of such BGO cylinder. As an example of the energy spectrum observed in the ions collisions where nucleus  $^{149}\text{Tb}$  is formed has been used (see Fig. 6). Approximately 100 lines from 60 keV up to 1500 keV are situated in the spectrum. On part (a) of Fig. 6 there are shown calculated unsuppressed and suppressed spectra without backward BGO cylinder. The backward BGO cylinder of 40 mm outer radius and 10 mm inner radius has been considered. The amount of inactive material between the Ge crystal and the cylinder is not easy to estimate. This material has been approximated with simple Al slab and the calculation for various Al slab thicknesses have been carried out. The dependence of the suppression factor on BCS cylinder length for various Al slab thickness are shown on part (b). From Fig. 6 it is clear that the material between the crystal and the BCS cylinder does not play an important role.

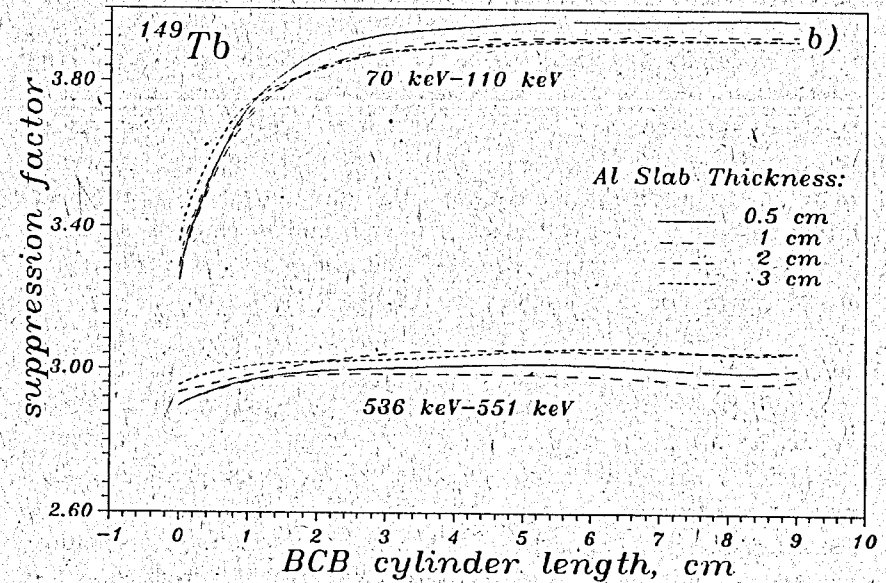
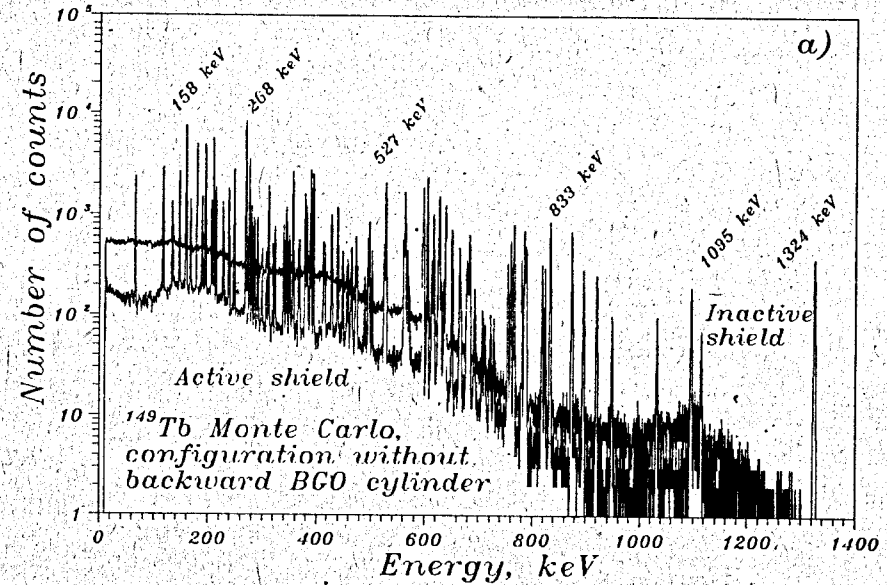


Figure 6: Part (a) shows the calculated suppressed and unsuppressed spectra of  $^{149}\text{Tb}$ . The dependence of suppression factor on BCS cylinder length and Al slab thickness is shown on part (b).

## 4.2. The influence of the nose part of CSS on total suppression efficiency.

Although the detection efficiency of NaI scintillator for the same geometry as in Fig. 2 is less than the efficiency of BGO, the NaI has been used in nose part of CSS (see Fig. 2). This fact is connected with a better signal/noise ration (particularly important for low  $\gamma$ -energy) and resolution ability of NaI. The back scattered  $\gamma$ -rays, which must be rejected by the nose part of CSS, have less energy than the small angle scattered ones and thus properties of NaI are desirable. On the opposite side the higher detection efficiency of BGO material is desirable for  $\gamma$ -rays scattered to the small angles. The difference of suppression efficiency for CSS with a nose from NaI or BGO was calculated. The apparent difference appears in the energy region above 1 MeV. It is possible to conclude, that the choice of the nose material does not influence the low energy region.

## 5. Conclusion

The use of Monte Carlo techniques allows to make satisfactory prediction of response function and suppression factor of various Compton suppression spectrometers. Two types of CSS have been investigated with typical high multiplicity  $\gamma$ -cascade source. The great emphasis has been put on absorption of Compton scattered photons in dead layers. The results of calculation based on EGS4 code system have been compared with experimental values. The agreement of measured and calculated data allows to predict the changes of suppression performance for modified configuration of CSS.

The modification, which has been considered is the addition of back BGO cylinder (BCB in Fig. 2) inside the detectors cavity. Since the suppression ability of BCB cylinder depends on energy structure of observed  $\gamma$ -rays a general conclusion is not possible. Nevertheless in case of  $^{149}\text{Tb}$  we have come to the conclusion that the increasing of suppression ability is not satisfactory (see Fig. 6 b). When the BCB scintillator is included the suppression ability of CSS in 70..110 keV region will increase from 3 up to 4.

## References

- [1] M. A. Riley, N. J. Ward, P. D. Forsyth, H. W. Griffiths, D. Howe, J. F. SharpeySchafer, J. Simpson, J. C. Lisle, E. Paul, P. Walker. *Proc. 5th Nordic Conf. on Nucl. Phys.*, Jyvaskyla, Finland, p.353, March 1984.
- [2] J. Kantele, P. Suominen. *Nuclear Instruments and Methods*, vol.41, p.41, 1966.
- [3] W. Michaelis, H. Kupfer. *Nuclear Instruments and Methods*, vol.56, p.181-188, 1967.
- [4] V.J. Orphan, N.C. Rasmussen. *Nuclear Instruments and Methods*, vol. 48, p.282, 1967.
- [5] B. Herskind. *Nuclear Physics*, A447(1985) p.395c-412c.
- [6] W.R. Nelson, H. Hirayama, W.O. Rogers. *Slac-report-265*, 1985.
- [7] GEANT2 User's Guide, CERN DD/EE/83 1
- [8] F.T. Avignone. *Nuclear Instruments and Methods*, vol.174, p.555-563 1980.
- [9] M. Moszynski, J.H. Bjerregard, J.J. Gaardhoje, B. Herskind, P. Knudsen, G. Sletten. *Nuclear Instruments and Methods*, A280 p.73-82, 1989.
- [10] W.O. Rogers. *Nuclear Instruments and Methods*, A277 p.535-548, 1984.
- [11] J.S. Dionisio, J.M. Lagrange, M. Pautrat, J.Vanhorenbeeck, Ch. Vieu. *Nuclear Instruments and Methods*, A271 p.527-542 1988.
- [12] J.S. Dionisio, H. Folger, Z. Meliani, C. Schuck, Ch.Vieu. *Nuclear Instruments and Methods*, A303 p.9-18 1991.

Received by Publishing Department  
on August 3, 1993.